Simple trapped-ion architecture for high-fidelity Toffoli gates

Simple trapped-ion architecture for high-fidelity Toffoli gates

Massimo Borrelli,[1] Laura Mazzola,[2,3] Mauro Paternostro,[3] and Sabrina Maniscalco[1,2]

[1]*CM-DTC, SUPA, EPS/School of Engineering & Physical Sciences, Heriot-Watt University, Edinburgh EH14 4AS, United Kingdom*

[2]*Turku Centre for Quantum Physics, Department of Physics and Astronomy, University of Turku, FI-20014 Turun yliopisto, Finland*

[3]*School of Mathematics and Physics, Queen's University, BT7 1NN Belfast, United Kingdom*

(Received 15 December 2010; revised manuscript received 11 May 2011; published 13 July 2011)

We discuss a simple architecture for a quantum TOFFOLI gate implemented using three trapped ions. The gate, which, in principle, can be implemented with a single laser-induced operation, is effective under rather general conditions and is strikingly robust (within any experimentally realistic range of values) against dephasing, heating, and random fluctuations of the Hamiltonian parameters. We provide a full characterization of the unitary and noise-affected gate using three-qubit quantum process tomography.

DOI: 10.1103/PhysRevA.84.012314 PACS number(s): 03.67.Lx, 32.80.Qk, 37.10.Ty

I. INTRODUCTION

In the quest for scalability of a quantum computing device, the role played by many-qubit gates is quite central. *Adequate sets* of gates have been identified that allow for the breakdown of complex computational networks in simpler tasks involving at most two qubits per time [1]. Unfortunately, the overhead in terms of the length of corresponding quantum circuits (i.e., the number of such elementary operations being required) soon overcomes the advantage provided by having to manage only two-body interactions. Multiqubit gates exist, able to bypass such a problem by requiring the simultaneous conditional evolution of three or more qubits. Among these, the TOFFOLI gate (whose unitary we label TOFFOLI) [2] is celebrated for its role in phase-estimation and error correction protocols [3], as well as in the quantum factorization algorithm [4]. Remarkably, the TOFFOLI gate has jumped across the field of computing, from classical to quantum, playing an important role in schemes for reversible classical computation [5]. The recent effort put in the task of harnessing a three-qubit TOFFOLI gate has been considerable. On one side, important experimental demonstrations on the practical realization of such gate have been reported [6,7]. On the other hand, significant improvement in the design of economic ways of implementing an n-qubit TOFFOLI gate have arisen from realizing that less resources are needed when using particles that live in higher-dimensional Hilbert spaces [8–10]. Interesting and compact architectures using the measurement-based paradigm for information processing have been also suggested [11].

Clearly, theoretical and experimental endeavors aiming at streamlining the realization of high-fidelity quantum gates and thus speeding-up the progress toward full scalability are extremely important and should be valued as such. In this paper, we present a compact protocol for the implementation of a high-fidelity three-qubit TOFFOLI gate in a trapped-ion architecture. Our scheme exploits an enlarged computational space consisting of three-level particles and an ancillary phononic mode [12,13]. While information is encoded only in two electronic states of each ion, their third levels are used as convenient *working spaces*, similarly to the phononic ancilla. In this respect, our algorithm is close in spirit to the work by Ralph *et al.* [8], although our protocol is different by construction, and to further proposals exploiting higher-dimensional particles for improved manipulation of the computational states [9]. As we shall prove, the use of an enlarged computational space and a simultaneous driving of multipole atomic transitions [14] allow a quite considerable reduction in the number of operations necessary to implement the three-qubit gate. Indeed, by adhering as much as possible to the parameters and working conditions of a single experimental setting, we show that our proposal requires roughly 44% of the operations needed in the seminal proof of principle provided by Monz *et al.* [6]. We thoroughly characterize the gate using three-qubit quantum process tomography (QPT) [15] performed using realistic working parameters and reveal its remarkable efficiency and robustness against leakage from the computational space, dephasing, heating, and laser-power fluctuations. We thus provide a possible platform for the experimental implementation of such a key gate in the design of quantum computing devices.

The paper is organized as follows. In Sec. II we give a full description of the protocol and compute the fidelity of the whole unitary process. In Sec. III we analyze how several sources of imperfections affect the process fidelity of the scheme. We numerically solve the Markovian master equation including heating and dephasing, and we statistically simulate the effect of a mismatch in the Rabi frequencies in the Hamiltonian model taking also into account the nonperfect preparation of the initial phononic state. In Sec. IV we summarize our findings.

II. THE PROTOCOL

Our system consists of $N = 3$ ions in a linear trap. We consider three energy levels $\{|l_j\rangle, |g_j\rangle, |e_j\rangle\}$ in a ladder configuration and their common phononic mode a (frequency ν). Potential candidates for such states are the electronic states $S_{1/2}(m = -1/2), S_{1/2}(m = 1/2), D_{5/2}(m = -1/2)\}$ in $^{40}Ca^{+}$ ions. The coupling between any pair of such levels is induced by controlled light-matter interactions at wavelength close to the $S_{1/2} \leftrightarrow D_{5/2}$ transition (wavelength 729 nm) [16]. The $|l_j(g_j)\rangle \leftrightarrow |e_j\rangle$ transition can be guided via quadrupole couplings while the $|l_j\rangle \leftrightarrow |g_j\rangle$ one can be driven by a far off-resonance Raman coupling through the fast-decaying $P_{3/2}$ level [17]. Both these cases are described in a unique framework where the internal and external degrees of freedom of an ion are coupled via the Hamiltonian (in the interaction picture)

$$\hat{H}_I(t) = (\hbar\Omega/2)\hat{\sigma}_{-}^{(\alpha\beta)} e^{-i\eta(\hat{a}e^{-i\nu t} + \hat{a}^{\dagger}e^{i\nu t}) - i(\omega_{\alpha\beta} - \omega_L)t} + \text{H.c.} \quad (1)$$

Here $\Omega \in \mathbb{R}$ is the Rabi frequency of the transition $|\alpha\rangle \leftrightarrow |\beta\rangle$ (with $\alpha,\beta = e,g,l$), $\hat{\sigma}_-^{(\alpha\beta)} = |\alpha\rangle\langle\beta|$, $\omega_{\alpha\beta}$ is the corresponding transition frequency, and η is the Lamb-Dicke parameter [17]. For a quadrupole transition, ω_L is the actual frequency of the field being used, while for a Raman transition this parameter is the difference between the frequencies of the two fields needed to off-resonantly couple $|l_j\rangle$ and $|g_j\rangle$ to the $P_{3/2}$ energy state. Finally, we have introduced the phononic annihilation (creation) operator $\hat{a}$ ($\hat{a}^\dagger$) of the quantized phononic mode. In the following, we exploit the flexibility of laser-induced trapped-ion dynamics that is achieved by tuning the laser-ion detuning $\delta_{\alpha\beta} = \omega_{\alpha\beta} - \omega_L$ [17]. In passing, we would like to remark that, as discussed above, our scheme relies on the use of both Raman and quadrupole transitions. While this is a perfectly realistic option, most recently employed for intracavity ion-photon interfaces [18], its realization may require a considerable technical effort compared to experiments that rely on only one of such coupling schemes.

In the well-known Lamb-Dicke [13] limit the Hamiltonian (1) can be greatly simplified and, depending on $\delta_{\alpha\beta}$, we can implement three different types of interaction. By setting $\delta_{\alpha\beta} = 0$ we realize a carrier coupling $\hat{H}_c = \hbar\Omega(1 - \eta^2 a^\dagger a)\hat{\sigma}_x^{(\alpha\beta)}$, which induces a complete spin flip without affecting the energy of the phonon mode. If we instead set $\delta_{\alpha\beta} = \nu$ we engineer the energy-conserving coupling $\hat{H}_r^{(\alpha\beta)}(\zeta) = \zeta\hat{a}\hat{\sigma}_+^{(\alpha\beta)} + \text{H.c.}$, where $\zeta = \hbar\eta(\Omega/2)$ and a phononic excitation is created (destroyed) upon annihilation (creation) of a spin quantum. Similarly, the choice $\delta_{\alpha\beta} = -\nu$ (corresponding to the tuning to the first blue sideband) induces the coupling $\hat{H}_b^{(\alpha\beta)}(\zeta) = \zeta\hat{a}^\dagger\hat{\sigma}_+^{(\alpha\beta)} + \text{H.c.}$ where spin and phononic excitations are simultaneously created or destroyed. We now show how to realize a TOFFOLI gate using the unitary evolution given by the Hamiltonian $\hat{H}_r$, together with properly arranged single-qubit operations preceding and following the dynamics induced by $\hat{H}_r$. We work in the single-excitation sector of the Hilbert space of the whole ionic string, including the phononic mode. Such operations will be required to guarantee that the state of the system remains within such subspace. Moreover, we should avoid any correlation between the internal degrees of freedom of the string and their vibrational one. Therefore, we have to enforce that the phononic mode, being initially prepared in $|0\rangle_a$, returns to this state when the gate is completed.

We are now in a position to describe the details of our protocol. First, we codify three qubits in the internal degrees of freedom of the ions by using the simple encoding scheme $(|0_1\rangle,|1_1\rangle) = (|g_1\rangle,|e_1\rangle)$, $(|0_j\rangle,|1_j\rangle) = (|g_j\rangle,|l_j\rangle)(j = 2,3)$. With this, we construct an eight-state basis for the three-qubit system as $\mathcal{B} = \{|000\rangle,|100\rangle,|010\rangle,|110\rangle,|001\rangle,|101\rangle, -i|011\rangle, -i|111\rangle\}_{123}$, where we have redefined the last two states so as to include an overall phase factor (the choice is made only to simplify our calculations). Our protocol begins with the realization of the single-qubit operations on the qubit 1-phononic mode system given by ($\tau = \pi/2\zeta$)

$$\hat{R}_A^+(\pi/2\zeta) = e^{i\hat{H}_b^{(eg)}(\zeta)\tau}, \quad \hat{R}_{B[C]}^-(\pi/2\zeta) = e^{i\hat{H}_r^{(l_e[g])}(\zeta)\tau}. \quad (2)$$

The first transformation in Eq. (2) excites the first blue sideband for the $|g_1\rangle \leftrightarrow |e_1\rangle$ transition while the remaining two embody the first red sideband excitations for the $|e_1\rangle \leftrightarrow |l_1\rangle$ and $|g_1\rangle \leftrightarrow |l_1\rangle$ passages. In order to work with the same phononic mode, we need laser fields with frequencies $\omega_L^A - \omega_{ge} = -\nu$, $\omega_L^B - \omega_{le} = \nu$, $\omega_L^C - \omega_{gl} = \nu$. In the subspace with at most a single excitation, it is straightforward to see that the composite operation $\hat{\mathcal{R}} = \hat{R}_C^-(\pi/2\zeta)\hat{R}_B^-(\pi/2\zeta)\hat{R}_A^+(\pi/2\zeta)$, operated on states having initially no phononic excitations, performs a logical $\hat{\sigma}_x$ gate in the space of the phononic mode, controlled by the spin state $|g_1\rangle$. That is $\hat{\mathcal{R}}(|g_1,0\rangle\,|e_1,0\rangle)^\mathsf{T} = (|g_1,1\rangle\,|e_1,0\rangle)^\mathsf{T}$. This operation encodes a logical qubit in the single-excitation states $\{|g_1,1\rangle,|e_1,0\rangle\}$. Therefore, we should consider the states of the extended system (with a single excitation overall) comprising the internal and external degrees of freedom of the string. This is seen, in our scheme, as the computational space of three logical qubits, one of which being embodied, in a sort of *dual rail* encoding, by $\{|0_L\rangle,|1_L\rangle\} \equiv \{|g_1,1\rangle,|e_1,0\rangle\}$ [15]. We now couple each ion to a field of frequency $\omega_L = \omega_{eg} + \nu$ at Rabi frequency Ω_j. The total interaction is described by [19]

$$\hat{H}_{TC} = \sum_{j=1}^{3}(\hbar\eta\Omega_j/2)\hat{a}|e_j\rangle\langle g_j| + \text{H.c.} \quad (3)$$

We let each of the single-excitation states mentioned above evolve under $\hat{H}_{\text{TC}}$ for a time t_T at which we turn Eq. (3) off and apply the gates forming $\hat{\mathcal{R}}$ in reverse order. This separates the state of the phononic mode from the spin state of ion 1. That is, we decode the logical qubit $\{|0_L\rangle,|1_L\rangle\}$ resetting the vibrational mode into $|0\rangle$ and remaining with just the ion-string computational states. The vibrational degrees of freedom can now be traced out without affecting the resulting gate,

$$\hat{\mathcal{U}}_T(t) = (\hat{\mathcal{R}}^\dagger \otimes \hat{\mathbb{1}}_{23})\exp[-(i/\hbar)\hat{H}_{\text{TC}}t_T](\hat{\mathcal{R}} \otimes \hat{\mathbb{1}}_{23}), \quad (4)$$

where $\hat{\mathbb{1}}_{23}$ is the identity operators in the tensor-product space of qubits 2 and 3. The main idea now is finding a time t_T such that $\hat{\mathcal{U}}_T(t)$ is as close as possible to the ideal gate TOFFOLI.

We first observe that there are four time scales associated with the dynamics at hand. Each of them is determined by the inverse of the Rabi frequencies of the processes involved in this scheme, that is, $\Theta_{123} = \hbar\eta(\sum_{j=1}^3 \Omega_j^2)^{1/2}$, $\Theta_{1j} = \hbar\eta(\Omega_1^2+\Omega_j^2)^{1/2}(j = 2,3)$, and $\Theta_1 = \hbar\eta\Omega_1$. The pedices used in such expressions identify the qubits that participate to the interaction with the phononic mode. It is thus clear that the quest for t_T is equivalent to the research of a set of suitable single-ion Rabi frequencies $\{\Omega_j\}$ such that our goal is achieved. An analytical/numerical optimization leads to the following relative ratios of coupling strengths $\Omega_1{:}\Omega_2{:}\Omega_3 = 1{:}\sqrt{143}{:}16$. With this at hand, at the optimal instant of time given by $t_T = \pi/\eta\Omega_1$, we find

$$\hat{\mathcal{U}}_T = \text{TOFFOLI} - 10^{-3}|110\rangle\langle 110| - 2\times 10^{-3}|001\rangle\langle 001|. \quad (5)$$

Needless to say, other choices can be found for the set of Rabi frequencies that achieve a gate close to TOFFOLI. However, the latter cannot be exactly achieved since one needs to maximize, simultaneously, eight trigonometric functions of incommensurate frequencies. Clearly, the only important parameter in our model is the ratio of the Rabi frequencies rather than their actual value. The time needed in order to implement the whole gate is $t_G = (\pi/\eta)[2\sum_{k=a,b,c}\Omega_k^{-1} + \Omega_1^{-1}]$, where Ω_k is the Rabi frequency of pulse $k = a,b,c$ in Eq. (2). In such a unitary picture, the implementation of Eq. (3)

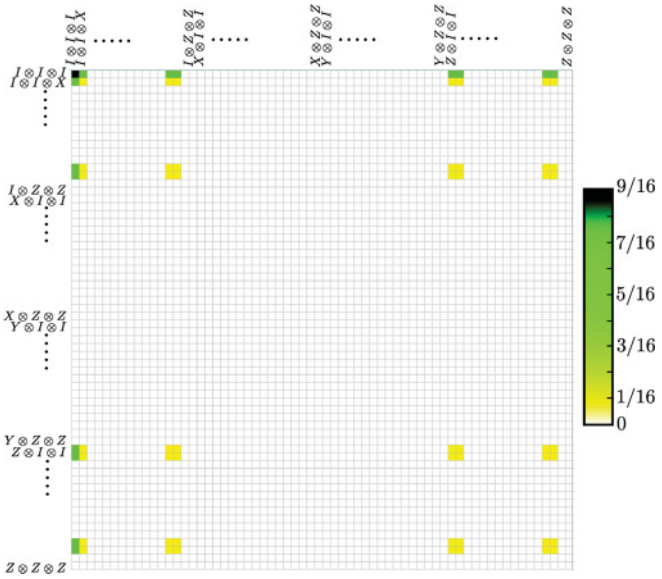

FIG. 1. (Color online) Reconstructed process matrix for $\hat{\mathcal{U}}_T$. The matrix is expressed in the three-qubit operator basis formed by $\{I \equiv \hat{\mathbb{1}}, X \equiv \hat{\sigma}_x, Y \equiv -i\hat{\sigma}_y, Z \equiv \hat{\sigma}_z\}$. We show the moduli of the matrix entries. The differences with respect to the elements of an ideal gate are $O(10^{-4})$.

for a time t_T is sufficient to implement a TOFFOLI-like gate over the logical target qubit $\{|0_L\rangle, |1_L\rangle\}$, which shows the striking economic nature of our proposal. Surely, the use of excited vibrational states would open the protocol to the effects of phononic heating and losses. The necessity of removing such excitations motivates the use of the encoding-decoding steps given by $\hat{\mathcal{R}}$.

To evaluate the quality of our proposal, the dynamics encompassed by the physical processes described so far should be characterized in a state-independent way. In what follows, we take an experiment-inspired approach and use QPT [15] as the tool to estimate the performance of the gate. Any completely positive N-qubit map $\Phi(t)$ is specified by a set of 4^N orthogonal operators $\{\hat{\mathcal{K}}_m\}$ such that $\Phi(t)\varrho(0) = \sum_{m,n} \chi_{mn}(t)\hat{\mathcal{K}}_m \varrho(0)\hat{\mathcal{K}}_n^\dagger$, where $\rho(0)$ is the initial density matrix of the system and we have introduced the $4^N \times 4^N$ time-dependent *process matrix* $\chi(t)$ that incorporates full information on the details of the evolution embodied by $\Phi(t)$. While a full description of the methodology needed to reconstruct $\chi(t)$ is given in the Appendix , here we remind that the process matrix allows us to evaluate the closeness of our protocol to the ideal TOFFOLI (having process matrix χ_T) by means of the *gate fidelity* $\mathcal{F}_g(t_G) = \mathrm{Tr}[\chi_T \chi(t_G)]$. In turn, this is useful to determine the average state fidelity $\overline{\mathcal{F}}_s(t_G) = [2^N \mathcal{F}_g(t_G)+1]/(2^N+1)$, which is obtained by averaging the fidelity between the ideal and the actual output states over all pure inputs [20]. In Fig. 1 we show the representation of the reconstructed process matrix in the tensorial operator-basis constructed by considering the single-qubit operators $\{\hat{\mathbb{1}}, \hat{\sigma}_x, -i\hat{\sigma}_y, \hat{\sigma}_z\}$. The entries of $\chi(t_G)$ differ from those of the ideal one by $O(10^{-4})$, showing the excellent quality of our gate, which has average *infidelity* $1 - \overline{\mathcal{F}}_s(t_G)$ as small as 10^{-5}.

III. ANLLYSIS OF IMPERFECTIONS

So far, we have considered only unitary evolutions. In order to provide an estimate of the efficiency of the gate under more realistic experimental conditions, we need to consider some of the most severe sources of imperfections in the ion-trap architecture addressed here [6]. In the following, we concentrate on quality-limiting effects of a nontechnical nature and take into account decoherence of the quantum information stored in the phononic mode given by the vibrational mode of the ion-string as well as heating due to the coupling between the phononic mode and a bath at finite temperature. By taking fast and intense optical pulses [6,17,21], the duration of sideband-resolved light-ion interactions necessary to implement $\hat{\mathcal{R}}$ can be made much shorter than the radiative lifetime of the ionic excited states, the heating of the center-of-mass mode, and the trap period. We thus neglect any decoherence effect occurring during the realization of single-ion gates, as achieved in Refs. [6,22], which are the experiments closer in spirit and design to our own proposal. At the same time, $\mathcal{R}$ should be applied to qubit 1 only. For a trapping potential having axial frequency $\sim$1.2 MHz [6], light pulses with small Gaussian waists of about 2.5 μm and an electro-optic deflector can be used to efficiently address individual ions with only a rather small addressing error. As stated in Ref. [6], the latter does not limit the accuracy of one-qubit operations at a fundamental level and mostly accounts for a technical imperfection. We thus consider the master equation

$$\partial_t \rho(t) = -i[\hat{H}_{\mathrm{TC}}, \rho(t)] - \frac{\kappa(\bar{n}+1)}{2}[\{\hat{a}^\dagger\hat{a}, \rho(t)\} - 2\hat{a}\rho(t)\hat{a}^\dagger] - \frac{\kappa\bar{n}}{2}[\{\hat{a}\hat{a}^\dagger, \rho(t)\} - 2\hat{a}^\dagger\rho\hat{a}] - \gamma[\hat{a}^\dagger\hat{a}, [\hat{a}^\dagger\hat{a}, \rho(t)]], \quad (6)$$

where $\rho(t)$ is the density matrix of the ionic string and the vibrational mode, κ is the heating rate, $\overline{n}$ is the mean number of phononic quanta of the bath at a given temperature, and γ is the dephasing rate. Analogously to the unitary case, the dynamical map $\mathcal{E}_H$ arising from Eq. (6) should be preceded and followed by the $\hat{\mathcal{R}}$ gate. That is, any initial state $\rho(0)$ of the three-ion system evolves until time t_G according to

$$\rho(t_G) = \hat{\mathcal{R}}^\dagger[\mathcal{E}_H(\hat{\mathcal{R}}\rho(0)\hat{\mathcal{R}}^\dagger)]\hat{\mathcal{R}}. \quad (7)$$

The resulting open-system dynamics implies, in principle, leakage from the computational space that would spoil the desired gate. In particular, the thermal evolution included in our assessment could lead to abandon the subspace where a is in state $|0\rangle_a$. The occurrence of such events and their influences are estimated by determining again the closeness of the map in Eq. (7) to the ideal gate. We have thus used QPT to quantify the average gate fidelity for the noise-affected evolution.

We have first considered the effects of heating of the phononic mode due to noisy electric potentials on the surface of the trap electrodes, resulting in an effective bath at nonzero temperature. We have taken $(\kappa^{-1}, \gamma^{-1}) = (140, 85)$ ms, values fully consistent with the center-of-mass mode and in line with the recent experiments [6], and considered $\overline{n}$ as increasing up to a maximum number of excitations equal to 5 [6]. We have then reconstructed the process matrix $\tilde{\chi}(t_G)$ and checked its resemblance to χ_T by calculating the discrepancy $|\tilde{\chi}(t_G) - \chi_T|$. Figure 2 shows the maximum value per row of

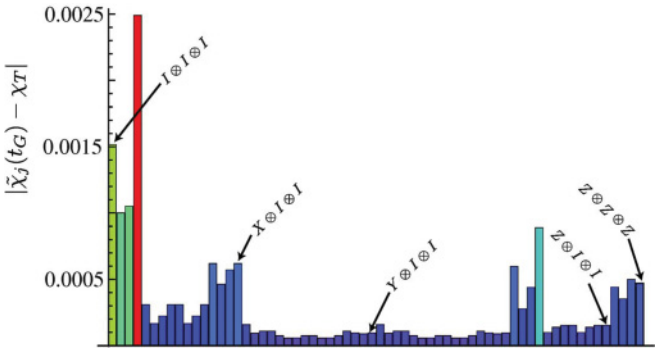

FIG. 2. (Color online) We take the largest entry per row in the discrepancy matrix $|\tilde{\chi}(t_G) - \chi_T|$ for $\overline{n} = 5$, $\gamma/\Omega = 10^{-3}$. We have highlighted the bars corresponding to some of the operator-basis elements.

such matrix. The largest deviation out of the 64 values gathered in this way is $\simeq 2.5 \times 10^{-3}$. In fact, the evaluation of the average gate fidelity leads to $\overline{F}_s = 0.994\,855$, which is 99.5% the value achieved for $\overline{n} = 1$. The remarkable insensitivity of the scheme to the effects of an increased mean phonon number is therefore proven. Our analysis allows us to conclude that $\mathcal{E}_H$ results in a dynamics that is well approximated by $\rho(t_G) \approx \rho_q(t_G) \otimes |0\rangle\langle 0|$, where $\rho_q(t_G)$ is the density matrix of the three-ion system. Our analysis allows us to conclude that results in a dynamics that is well approximated by Our next step is the evaluation of the dephasing effects, which we performed by solving Eq. (6) for $\overline{n} = 1$, $\kappa^{-1} = 140$ ms, and growing γ. Figure 3 (circles) shows the quasi-independence of the effective gate from a raise of γ by almost one order of magnitude from the value estimated in Ref. [6] ($1-\overline{\mathcal{F}}_s \in [10^{-5}, 0.07]$ for $\gamma/\Omega \in [0, 12.5] \times 10^{-3}$).

As remarked above, a key point in our proposal is the maintenance of precise ratios of the Rabi frequencies of the operations involved in the construction of $\hat{\mathcal{U}}_T$. We know that, in a real experimental setup, such a task might be quite

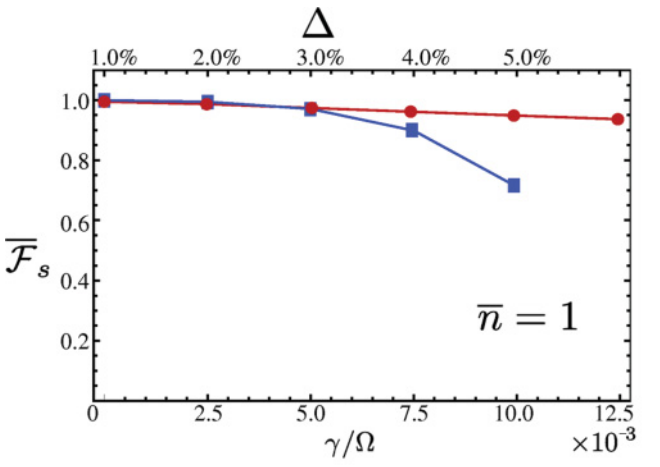

FIG. 3. (Color online) Bottom horizontal axis and circular points: Average state fidelity for $\hat{\mathcal{U}}_T$ vs γ/Ω. At $\gamma = 0$, it is $\overline{\mathcal{F}}_s = 0.999\,988$, while for the larger dephasing rate that we have considered we have $\overline{\mathcal{F}}_s > 0.93$. Top horizontal axis and squared points: Average gate fidelity for $\hat{\mathcal{U}}_T$ vs the variance Δ of the distribution taken for the amplitudes of lasers. The lines are guides for the eye.

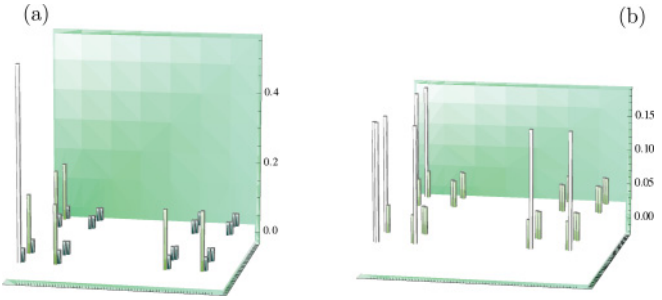

FIG. 4. (Color online) (a) Moduli of the real part of the process matrix associated with the unitary gate $\hat{\mathcal{U}}_T$. The top-left corner of the matrix corresponds to the operator-basis element $I \otimes I \otimes I$. (b) Same as in panel (a) but for the imaginary parts of the χ matrix.

tricky to accomplish and lasers fluctuations can, in principle, jeopardize the stability required in the proposed scheme. Since a unique analytical description of such a technical imperfection is still missing we have adopted a statistical approach solving Eq. (6) again, this time treating the Ω_j's as stochastic variables which randomly oscillate around the corresponding ideal values. More in detail, we have taken $\Omega_j^{'} = \Omega_j + \delta\Omega_j$, with $\delta\Omega_j/\Omega_j$ a uniformly distributed zero-mean variable with variance $\Delta \in [1,5]\%$. Using a sample of 500 randomly drawn values of $\delta\Omega_j$ and evaluating the corresponding dynamical evolution, we have calculated the sample-averaged $\overline{\mathcal{F}}_s$. In the worst-case scenario given by $\Delta = 5\%$ (which anyhow overestimates current experimental capabilities), we have achieved an average fidelity of $\simeq 71\%$. Finally, we have estimated the influence that a residual thermal character of the initial vibrational state has on our scheme. By preparing a in a low-temperature thermal state with a mean number of excitations up to 10^{-1}, we have found that the leakage from the computational space remains quite negligible, with a gate fidelity that in the unitary case is never smaller than 0.901. The analysis has been repeated also in the open-system case, finding a fidelity equal to 0.8962 for $\overline{n} = 5$ and $\gamma = 85$ ms, while $\overline{\mathcal{F}}_s = 0.6396$ for the case of fluctuating Rabi frequencies with $\Delta = 5\%$. A quite good robustness of the gate against such a state-preparation error is thus demonstrated.

Any multiqubit gate can be decomposed as a concatenation of single-qubit and two-qubit operations belonging to a set of universal quantum gates. In particular, it is known that such a concatenation for the three-qubit TOFFOLI gate involves six control-NOT gates and nine single-qubit rotations. [1]. In order to prove the advantages of our scheme, with respect to a more traditional quantum circuit approach, it is reasonable to compare the fidelity achieved by our protocol to what is found by decomposing TOFFOLI with state-of-the-art two-qubit gates. In doing so we refer to the work reported in [23]. Here a fidelity of 0.85 was obtained concatenating two control-NOT gates. By ascribing the largest source of imperfections to the two-qubit gates in the decomposition, TOFFOLI would be realized with 0.614 fidelity. By extrapolating the behavior shown by the squared points in Fig. 3, $\Delta \sim 5.5\%$ is required to match this value, which is a very pessimistic estimate for the fluctuations of the Rabi frequencies.

Recent experiments have demonstrated schemes to implement two-qubit gates unaffected by intrinsic error mechanisms

[24]. While the circuit decomposition of the TOFFOLI gate based on this sort of building blocks is not straightforward, the use of such gates might also lead to a more robust two-qubits decomposition.

IV. CONCLUSIONS

We have discussed a scheme for the implementation of a high-fidelity three-qubit TOFFOLI gate that requires, in principle, about 44% of the total number of operations needed by a very recent experimental demonstration in a trapped-ion system. Despite using a work-space larger than that of three qubits, our protocol is remarkably robust and affected by only negligible leakage from the computational space. It enjoys the gate-catalysis effects provided by the use of higher-dimensional information carriers. Using QPT, we have characterized the performances of the gate adopting parameters extracted from cutting-edge experiments. We have estimated the influence of some of the most relevant causes of imperfections in the setup at hand, finding quite a striking resilience. Economic schemes such as ours are important in the design of experimental architectures for trapped-ion quantum computing to be promptly implemented in state-of-the-art settings [6,25].

ACKNOWLEDGMENTS

M.B., L.M., and S.M. acknowledge partial financial support from the Emil Aaltonen Foundation, the Finnish Cultural Foundation, and the Magnus Ehrnrooth Foundation. M.P. is grateful to the OQSE group, University of Turku, for the hospitality and acknowledges financial support from EPSRC (EP/G004579/1) and the British Council.

APPENDIX: QUANTUM PROCESS TOMOGRAPHY

The complete characterization of a general completely positive dynamical map Φ_N over an N-qubit register can be performed by relying on the framework of QPT [15]. By using this formalism it is possible to determine of a complete set of orthogonal operators $\{\hat{\mathcal{K}}_m\}$ over which one can perform the decomposition of each Kraus operator $\hat{K}_i = \sum_m e_{im}\hat{\mathcal{K}}_m$ so as to get

$$\Phi_N \varrho = \sum_{m,n} \chi_{mn} \hat{\mathcal{K}}_m \varrho \hat{\mathcal{K}}_n^\dagger, \tag{A1}$$

where the *channel matrix* $\chi_{mn} = \sum_i e_{im} e_{in}^*$ has been introduced. This is a pragmatically very useful result as it shows that it is sufficient to consider a fixed set of operators, whose knowledge is enough to characterize a channel through the matrix χ. We consider the specific case of a system of three qubits. The action of Φ over a generic element of a basis in the space of the $2^3 \times 2^3$ matrices can be determined by knowing the action of Φ over the fixed set of states constructed as the tensor product of the single-qubit ensemble of states $|0\rangle,|1\rangle,|+\rangle = (1/\sqrt{2})(|0\rangle + |1\rangle)$ and $|+_y\rangle = (1/\sqrt{2})(|0\rangle + i|1\rangle)$ as follows. Let us illustrate this argument by means of a single-qubit example. The action of Φ_1 on the generic element $|n\rangle\langle m|$ of a single-qubit density matrix $(n,m = 0,1)$ can be reconstructed as

$$\begin{aligned}\Phi_1(|n\rangle\langle m|) = {} & \Phi_1(|+\rangle\langle +|) + i\,\Phi_1(|+_y\rangle\langle +_y|) \\ & - (i+1)[\Phi_1(|n\rangle\langle n|) + \Phi_1(|m\rangle\langle m|)]/2. \end{aligned} \tag{A2}$$

The argument can be easily extended to the case of three qubits, involving $4^3 = 64$ ensemble states. Therefore, it is straightforward to see that all the entries $\varrho_k = |n_1,n_2,n_3\rangle\langle m_1,m_2,m_3|$ $(n_j,m_j = 0,1$ with $k = 1,..,64)$ of an 8×8 density matrix can be found via state tomography of 64 fixed states. Clearly, $\Phi(\varrho_j) = \sum_k \lambda_{jk}\varrho_k$ as $\{\varrho_k\}$ form a basis. From the above discussion we have

$$\Phi_3 \varrho_j = \sum_{m,n} \hat{\mathcal{K}}_m \varrho_j \hat{\mathcal{K}}_n^\dagger \chi_{mn} = \sum_{m,n,k} \beta_{jk}^{mn} \varrho_k \chi_{mn} = \sum_k \lambda_{jk} \varrho_k, \tag{A3}$$

where we have defined $\hat{\mathcal{K}}_m \varrho_j \hat{\mathcal{K}}_n^\dagger = \sum_k \beta_{jk}^{mn} \varrho_k$ so that we can write

$$\lambda_{jk} = \sum_{m,n} \beta_{jk}^{mn} \chi_{mn}. \tag{A4}$$

The complex tensor β_{jk}^{mn} is set once we make a choice for $\{\hat{\mathcal{K}}_i\}$ and the λ_{jk}'s are determined from a knowledge of $\Phi\varrho_j$. By inverting Eq. (A4), we get the channel matrix χ and characterize the map. Let $\hat{\mathcal{V}}^\dagger$ be the operator diagonalizing the channel matrix. Then it is straightforward to prove that if D_i are the elements of the diagonal matrix $\hat{\mathcal{V}}^\dagger \chi \hat{\mathcal{V}}$, then $e_{im} = \sqrt{D_i}\hat{V}_{mi}$, so that

$$\hat{K}_i = \sqrt{D_i} \sum_j \hat{\mathcal{V}}_{ji} \hat{\mathcal{K}}_j. \tag{A5}$$

As discussed in detail in the body of our paper, we have determined the process matrix of our TOFFOLI gate, finding striking closeness with the ideal case. In Fig. 4 we provide further details of such reconstruction, by showing the moduli of both the real and imaginary parts of the χ matrix elements. Moreover, we have computed the full set of Kraus operators corresponding to the map associated with the gate $\hat{\mathcal{U}}_T$ presented in the main body of the paper, finding

$$\hat{K}_1 = \begin{pmatrix} 1 & -5.55\times10^{-17} & 0 & 0 & 0 & 0 & 0 & 0 \\ -5.55\times10^{-17} & 1 & 0 & 0 & 0 & 0 & 0 & 0 \\ 0 & 0 & 1 & -1.11\times10^{-16} & 0 & 0 & 0 & 0 \\ 0 & 0 & -1.11\times10^{-16} & 1 & 0 & 0 & 0 & 0 \\ 0 & 0 & 0 & 0 & 0.999 & -5.55\times10^{-17} & 0 & 0 \\ 0 & 0 & 0 & 0 & -5.55\times10^{-17} & 0.998 & 0 & 0 \\ 0 & 0 & 0 & 0 & 0 & 0 & -3.33\times10^{-16} & 1 \\ 0 & 0 & 0 & 0 & 0 & 0 & 1 & -4.44\times10^{-16} \end{pmatrix}, \tag{A6}$$

with $\hat{K}_j = \mathbf{0}$ ($j = 2, \ldots, 64$). Clearly, the fact that only a single Kraus operator is different from the null matrix is the result of the unitarity of the process at hand. Beside tiny elements no larger than 10^{-16} (likely arising from small computational inaccuracies), $\hat{K}_1$ turns out to be identical to Eq. (6) in the main body of the paper.

[1] A. Barenco, C. H. Bennett, R. Cleve, D. P. DiVincenzo, N. Margolus, P. Shor, T. Sleator, J. A. Smolin, and H. Weinfurter, Phys. Rev. A **52**, 3457 (1995).

[2] T. Toffoli, in *Automata, Languages and Programming*, edited by J. W. de Bakker and J. van Leeuwen (Springer, New York, 1980).

[3] D. G. Cory, M. D. Price, W. Maas, E. Knill, R. Laflamme, W. H. Zurek, T. F. Havel, and S. S. Somaroo, Phys. Rev. Lett. **81**, 2152 (1998).

[4] P. W. Shor, SIAM J. Sci. Stat. Comput. **26**, 1484 (1997).

[5] E. Fredkin and T. Toffoli, Int. J. Theor. Phys. **21**, 219 (1982).

[6] T. Monz, K. Kim, W. Hänsel, M. Riebe, A. S. Villar, P. Schindler, M. Chwalla, M. Hennrich, and R. Blatt, Phys. Rev. Lett. **102**, 040501 (2009).

[7] B. P. Lanyon, M. Barbieri, M. P. Almeida, T. Jennewein, T. C. Ralph, K. J. Resch, G. J. Pryde, J. L. O' Brien, A. Gilchrist, and A. G. White, Nat. Phys. **5**, 134 (2009).

[8] T. C. Ralph, K. J. Resch, and A. Gilchrist, Phys. Rev. A **75**, 022313 (2007).

[9] J. Fiurášek, Phys. Rev. A **73**, 062313 (2006); R. Ionicioiu, T. P. Spiller, and W. J. Munro, *ibid.* **80**, 012312 (2009).

[10] S. S. Ivanov and N. V. Vitanov, e-print arXiv: 1106.0270v1.

[11] M. S. Tame, M. Paternostro, M. S. Kim, and V. Vedral, Phys. Rev. A **73**, 022309 (2006).

[12] A. scheme for a trapped-ion controlled-controlled-phase gate has been presented in C.-Y. Chen and S.-H. Li, Eur. Phys. J. D **41**, 557 (2007). Such a proposal differs from ours in both the role played by a and the necessity of two extra local operations on the target qubit for the achievement of Toffoli.

[13] J. I. Cirac and P. Zoller, Phys. Rev. Lett. **74**, 4091 (1995).

[14] K. Mølmer and A. Sørensen, Phys. Rev. Lett. **82**, 1835 (1999).

[15] M. A. Nielsen and I. L. Chuang, *Quantum Computation and Quantum Information* (Cambridge University Press, Cambridge, 2000).

[16] The degeneracy of $|l_j\rangle$ and $|g_j\rangle$ can be split by a magnetic field of 1.5 G, giving rise to a difference in frequency of about 4.2 MHz.

[17] D. Leibfried, R. Blatt, C. Monroe, and D. WIneland, Rev. Mod. Phys. **75**, 281 (2003).

[18] A. Stute, B. Casabone, B. Brandstätter, D. Habicher, P. O. Schmidt, T. E. Northup, and R. Blatt, e-print arXiv:1105.0579v1.

[19] M. Tavis and F. W. Cummings, Phys. Rev. **170**, 379 (1968).

[20] J. L. O'Brien, G. J. Pryde, A. Gilchrist, D. F. V. James, N. K. Langford, T. C. Ralph, and A. G. White, Phys. Rev. Lett. **93**, 080502 (2004); A. Gilchrist, N. K. Langford, and M. A. Nielsen, Phys. Rev. A **71**, 062310 (2005).

[21] P. J. Lee, K.-A. Brickman, L. Deslauriers, P. C. Haljan, L.-M. Duan, and C. Monroe, J. Opt. B **7**, S371 (2005).

[22] S. Gulde, M. Riebe, G. P. Lancaster, C. Becher, J. Eschner, H. Häffner, F. Schmidt-Kaler, I. L. Chuang, and R. Blatt, Nature (London) **421**, 48 (2003).

[23] M. Riebe, K. Kim, P. Schindler, T. Monz, P. O. Schmidt, T. K. Korber, W. Hansel, H. Haffner, C. F. Roos, and R. Blatt, Phys. Rev. Lett. **97**, 220407 (2006).

[24] Benhelm, G. Kirchmair, C. F. Roos, and R. Blatt, Nat. Phys. **4**, 463 (2008).

[25] E. E. Edwards, S. Korenblit, K. Kim, R. Islam, M.-S. Chang, J. K. Freericks, G.-D. Lin, L.-M. Duan, and C. Monroe, e-print arXiv:1005.4160v1; G.-D. Lin, C. Monroe, and L.-M. Duan, e-print arXiv:1011.5885v1.